

RNiO₃ perovskites (R = Pr, Nd): Nickel valence and the metal-insulator transition investigated by x-ray-absorption spectroscopy

M. Medarde* and A. Fontaine

Laboratoire pour l'Utilisation du Rayonnement Electromagnétique, Bâtiment 209 D, 91405 Orsay, France

J. L. García-Muñoz and J. Rodríguez-Carvajal

Institut Laue-Langevin, 156X, 38042 Grenoble, France

M. de Santis, M. Sacchi, and G. Rossi

Laboratoire pour l'Utilisation du Rayonnement Electromagnétique, Bâtiment 209 D, 91405 Orsay, France

P. Lacorre[†]

IBM Research Division, Almaden Research Center, 650 Harry Road, San José, California 95120-6099

(Received 13 July 1992)

The strongly correlated and nominally trivalent Ni oxides RNiO₃ (R = Pr, Nd) show a sharp metal to insulator transition at $T_{M-I} = 135$ and 200 K, respectively. Rare-earth (3*d*), Ni (1*s*, 2*p*), and O (1*s*) x-ray absorption measurements have been performed above and below the transition temperature in order to investigate (a) the valence of Ni and O atoms and (b) the changes in the electronic structure across the transition. Our results suggest that, in contrast to hole-doped Ni_{1-x}Li_xO and La_{2-x}Sr_xNiO_{4+δ}, the electronic structure is characterized by a strongly hybridized ground state of mainly 3*d*⁷ character. The differences between the absorption edges at low (insulating) and high (metallic) temperatures are discussed in terms of the possible mechanisms responsible for the metal-insulator transition.

I. INTRODUCTION

Since the absence of Cu³⁺ “formal valence” was established in high-temperature superconducting cuprates such as YBa₂Cu₃O_{6.9}, La_{2-x}Sr_xCuO₄, or Bi₂CaSr₂Cu₃O_{8+δ}, there has been a great deal of interest in the oxidation state of Cu and other late transition metals (TM's) in oxides. Apart from Cu, great effort has been devoted to investigate the hole-doped nickelates (Li-doped NiO, Sr-doped La₂NiO₄) (Refs. 1 and 2) and, in general, all the TM oxides showing unusual 3*d*-metal valencies such as Cu³⁺ (NaCuO₂, LaCuO₃)^{3,4} Ni³⁺ (LaNiO₃)⁵ or Fe⁴⁺ (SrFeO₃)^{6,7}

Thus, recently, Kuiper *et al.*¹ suggested that the “formal” charge states Ni_{1+2x}Li_xNi_x³⁺O²⁻ for Li-doped NiO were actually wrong. As in the doped superconducting copper oxides, oxygen 1*s* x-ray absorption (XAS) experiments demonstrated that the holes compensating the Li¹⁺ impurity charge in Li_xNi_{1-x}O (0 ≤ *x* ≤ 0.5) have O 2*p* character rather than Ni 3*d* character. A similar result has been found in polarization-dependent XAS measurements on the electrical insulator La₂NiO_{4+δ} after being doped with Sr (La_{2-x}Sr_xNiO₄, 0 ≤ *x* ≤ 1.15).² However, the conclusions derived by van Elp⁸ from XPS (x-ray photoelectron spectroscopy) and BIS (bremsstrahlung isochromate spectroscopy) measurements concerning the character and symmetry of the induced holes in Li-doped CoO are in disagreement with recent XAS results reported by de Groot.⁹ Whereas van Elp suggests O 2*p* character (*d*⁷ \bar{L} [³T₁] symmetry) when 0 < *x* ≤ 0.2, de Groot proposes Co 3*d* character (3*d*⁶[¹A₁] symmetry) for the same

range of concentrations.

There is also no general agreement concerning systems such as LiNiO₂, LaCuO₃, and LaNiO₃, where the electronic state of the TM cations is still very controversial.^{8,10-13} LiNiO₂ is probably the most deeply investigated among these compounds. In the literature, several models with different spin and charge states for the Ni and O ions have been proposed to explain various experimental results. In particular, Goodenough, Wickham, and Croft¹⁴ suggested a Ni³⁺ low-spin state to explain the results of crystallographic and magnetic measurements, whereas Kuiper *et al.*¹ propose Ni²⁺ antiferromagnetically coupled with O 2*p* holes to interpret the results of core-level x-ray spectroscopies. It is important to point out that rigorous structural studies have not been reported in previous investigations, presumably due to the difficulties involved in achieving an accurate control of the Li and O stoichiometry. This is, in our opinion, a very crucial point which has to be solved in order to get a solid physical interpretation.

On the other hand, some of the theoretical efforts made in recent years for describing the differences between the metallic and the insulating state have been recently condensed in a unified framework Zaanen-Sawatzky-Allen theory.¹⁵ The most interesting feature of this approach is that, using only a few parameters (fundamental electronic energies), it has been shown to be able to account for the electronic behavior of a great number of 3*d* TM oxides.¹⁶ The involved parameters are (i) the *d-d* Coulomb interaction *U* (which also includes exchange) defined as the excitation energy necessary to produce charge fluctuations of the type *d*_{*i*}^{*n*}*d*_{*j*}^{*n*} → *d*_{*i*}^{*n*-1}*d*_{*j*}^{*n*+1} (here *i* and *j* label 3*d*-metal

sites and n the $3d$ -orbital occupation); (ii) the charge-transfer energy Δ , defined as $E(d_i^{n+1}d_j^n\bar{L})-E(d_i^n d_j^n)$, where \bar{L} stands for an anion (ligand) hole; and (iii) the ligand (W) and metal (w) one-electron bandwidths. Thus, by comparing the corresponding values of U , Δ , W , and w , TM oxides can be easily classified as insulators (Mott-Hubbard if $W < U < \Delta$ and charge transfer if $W < \Delta < U$) or metals (low U if $U < w$ and low Δ if $\Delta < W$).

Very recently, Mizokawa *et al.*¹⁷ pointed out that with increasing atomic number or increasing formal valence of the metal element, Δ systematically decreases. These authors stressed that Δ may become very small or negative with unusually high valencies such as Fe^{4+} , Ni^{3+} , or Cu^{3+} . In this case, the $d^{n+1}\bar{L}$ configuration should be equally or even more favorable than the $3d^n$ one. The expected charge fluctuations in the metallic state are of the type $d^{n+1}\bar{L}d^{n+1}\bar{L} \rightarrow d^{n+1}d^{n+1}\bar{L}^2$ and the existence of a gap is only possible in the presence of O $2p$ -O $2p$ hole correlations strong enough to split the O $2p$ band (p - p gap). This seems to be the case for the insulator NaCuO_2 , where XPS measurements and the cluster calculation reported by Mizokawa *et al.*¹⁷ give a value of $\Delta = -2(\pm 1)$ eV. Following these authors, the gap in NaCuO_2 is neither of the Mott-Hubbard type nor of the charge-transfer type, but of the p - p type.

The perovskite PrNiO_3 , one of the compounds reported in this paper, was recently synthesized for the first time by Lacorre *et al.*¹⁸ This one and the other RNiO_3 perovskites ($R = \text{La, Pr, Nd, Sm, Eu, Lu, Y}$) form a very interesting series because (i) Ni shows a high oxidation state and (ii) they exhibit a metal-insulator (M - I) transition ($R \neq \text{La}$) where T_{M-I} is controlled by the size of the rare earth.¹⁸ Thus, whereas LaNiO_3 remains metallic, $T_{M-I} = 135, 200, 400,$ and 480 K for $R = \text{Pr, Nd, Sm, and Eu}$, respectively. LuNiO_3 and YNiO_3 are insulators below 500 K, but a M - I transition is expected to take place at higher temperatures. The M - I transition is accompanied by subtle, electronically induced, structural changes involving the Ni-O-Ni angles and the Ni-O distances.¹² The mechanism controlling the gap opening in the low-temperature insulating phase is controversial at the present time. Torrance *et al.* propose a charge-transfer gap¹⁶ but the high formal valence of Ni ($3+$) makes these perovskites good candidates to show a p - p gap, as suggested by Mizokawa *et al.*¹⁷

Although it is evident that spectroscopic techniques such as XAS, XPS, or BIS are more suitable to probe electronic states, the results of the crystallographic analysis by high-resolution neutron powder diffraction and the valence-bond method¹⁹ (VBM) suggest that the classical assumption R^{3+} , Ni^{3+} (low spin), and O^{2-} is a good starting point for an understanding of the electronic structure of these systems.¹² This idea is also supported by the magnetic behavior found in these compounds. Whereas metallic LaNiO_3 remains paramagnetic in all the temperature range studied, the M - I transition in PrNiO_3 and NdNiO_3 is accompanied by a sudden formation of three-dimensional (3D) ordered $S = \frac{1}{2}$ magnetic moments at the Ni sites.²⁰ The insulating regime has a magnetic ground state consisting of an unusual commens-

urate spin-density wave (SDW). The spin periodicity involves four Ni-Ni distances along the three directions $\langle 100 \rangle$ of the pseudocubic axes. This implies the symmetrical coexistence of ferro- and antiferromagnetic interactions which can be explained in terms of a nonuniform orbital distribution of the single low-spin- $\text{Ni}^{3+} e_g$ electron.²¹ This type of spin arrangement, whose existence is clearly confirmed by the behavior of the paramagnetic rare earth in the field created by the 3D ordered Ni magnetic moments, is unprecedented in a perovskite structure.

The appearance of this SDW is in principle open to other interpretations, namely, those requiring a ground state with a great amount of $3d^8\bar{L}$ character. However, the $3d^8\bar{L}$ state implies the existence of nonzero magnetic moments at the O sites and, in consequence, complicates the situation somewhat. Although in some oxides the existence of a nonzero spin density at the O sites has been clearly established,²² the observed magnetic intensities in RNiO_3 compounds are, at the present time, very difficult to conciliate with the presence of localized magnetic moments in the O sites.²⁰

Last but not least, we want to emphasize that PrNiO_3 and NdNiO_3 are the only nondoped Ni perovskites where (i) the electronic localization and the Néel state take place at the same temperature ($T_N = T_{M-I}$) and (ii) the formation of a unusual SDW in the insulating state has been reported. For SmNiO_3 and EuNiO_3 , T_{M-I} is respectively 400 and 480 K, whereas the Néel temperatures are dramatically lower (225 and 205 K, respectively). The magnetic structure of the Sm and Eu compounds have not yet been studied, but it would be very interesting to investigate whether it is of the same type found in the $T_N = T_{M-I}$ compounds. This information is fundamental to establish the relation between structural, magnetic, and electronic properties and to advance the understanding of the mechanism responsible of the M - I transition.

In the present work we report O ($1s$), Ni ($1s, 2p$), and R ($3d$) x-ray absorption measurements for RNiO_3 ($R = \text{Pr, Nd}$) samples. As will be discussed below, these data strongly suggest the presence of a highly hybridized ground state of mainly $3d^7$ character. The different possibilities for the mechanism of the electronic transition are also discussed.

II. EXPERIMENT

Polycrystalline samples of RNiO_3 ($R = \text{Pr, Nd}$) were used in the present work. The preparation method is described by Lacorre *et al.* in Ref. 18. Previous x-ray and neutron-diffraction characterization showed the compounds to be very well crystallized and virtually free of structural defects.¹² A very small amount of NiO (0.35% of the total weight for PrNiO_3 and 3% for NdNiO_3) was the only detected impurity. The XAS measurements were made in Orsay at LURE (Laboratoire pour l'Utilisation du Rayonnement Electromagnétique) using the synchrotron radiation emitted by the DCI (1.85 GeV) and Super-ACO (0.8 GeV) storage rings.

Ni $1s$ -edge XAS experiments were performed in

transmission mode. This method is more sensitive to the bulk properties of the material but requires a very good particle-size homogeneity. In this case, samples were ground (to become a fine powder) in an agatha mortar, filtered, and spread between two kapton tapes. The spectra were recorded in the time-resolved x-ray spectrometer D11 at DCI using an asymmetrically cut (-12°) Si (311) bent crystal. The energy resolution was better than 1 eV at 9 KeV. The low-temperature experiments were carried out with an He cryostat equipped with a temperature controller (stability better than 1 K).

The Ni $2p$ and rare-earth $3d$ edges were measured at Super-ACO in the SA22 experimental station using a double-crystal monochromator equipped with beryl crystals. The resolution for this instrument is better than 0.4 at 850 eV. The spectra were recorded at a vacuum of 10^{-9} Torr in the total electron yield mode. Samples were compacted and heated at 800°C in air for 2 days in order to produce rods which can be scraped in vacuum. Thermogravimetric analysis showed that this thermal treatment does not produce any O loss. Samples were measured at room temperature (RT) before and after scraping with a diamond file. The energy scale was calibrated by comparison with data from van der Laan *et al.*²³

O $1s$ edges were measured at Super-ACO on the SA7 experimental station using a plane-grating monochromator. The resolution for this instrument is 0.35 at 500 eV. The spectra were recorded at a vacuum of 10^{-9} Torr in the total electron yield mode. The energy-dependent photon flux due to the contamination of the optical elements was found to be negligible in the O $1s$ region. The samples were prepared in the same way as for the Ni $2p$ -edge experiments. Measurements were made at room temperature and at 77 K, using in the latter case a liquid-N₂ refrigerated cold finger. Spectra were systematically taken before and after scraping the samples in vacuum. The energy scale was calibrated by comparison with data of Kuiper *et al.*¹

III. RESULTS

A. O $1s$ edge

Figure 1 shows the O $1s$ edges of LaNiO₃, PrNiO₃, and NdNiO₃ measured at RT. At high energies, the oscillations

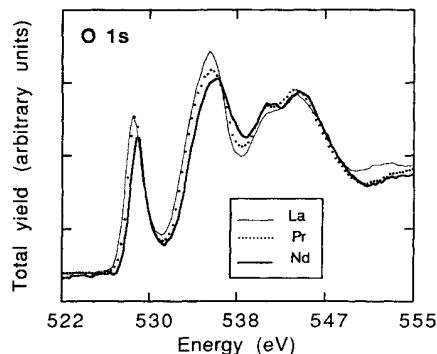


FIG. 1. Room-temperature O $1s$ edges of LaNiO₃, PrNiO₃ and NdNiO₃.

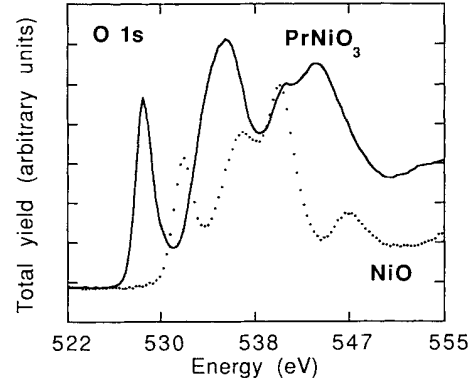


FIG. 2. Room-temperature O $1s$ edges of PrNiO₃ and NiO.

tions in the absorption cross section above 538.5 eV are due to transitions to continuum states.² The nice overlap of the PrNiO₃ and NdNiO₃ spectra in this region was used as criterion for normalization due to the strong similarities between the O environment in both compounds. Differences between LaNiO₃ and PrNiO₃ or PrNiO₃ at $E > 547$ eV are probably due to the slightly different symmetry of the La (rhombohedral), and Pr, Nd (orthorhombic) perovskites.¹⁸

The structures between 532 and 538.5 eV are due to transitions to oxygen $2p$ states hybridized with Ni($4s, 4p$) and R ($5d, 4f$) states.^{2,23} The decrease of the prominent peak at 536 eV going from La to Nd can be tentatively associated with the filling of the $4f$ rare-earth orbitals.

Finally, in the low-energy region, the most important feature is the sharp and intense prepeak situated at 528.4 (La), 528.6 (Pr), and 528.8 (Nd) eV (see Table I). Using the normalization procedure described above, its integrated intensity decreases going from La to Pr (9%) and Nd (20%). A similar structure is also present in the NiO O $1s$ edge (see Fig. 2), but its position (532 eV) is about 3 eV higher than the RNiO₃ prepeak. This feature, which has been also found in the O $1s$ edges of the other transition-metal monoxides,²³ is due to the O $2p$ weight in states of predominantly Ni $3d$ character.

Figure 3 shows the RT and 77-K O $1s$ edges of (a) PrNiO₃ and (b) NdNiO₃. Due to the small differences between the high- and low-temperature spectra, several measurements were made at low temperature to be sure that the observed effects are not due to surface contamination (enhanced by cooling). A small increase of the integrated intensity of the prepeak (about 3%) is detected in both cases when the sample goes from the metallic to the insulating state. A simultaneous decrease of the 536-eV structure was also systematically observed on cooling.

TABLE I. Absolute energies (eV) and integrated intensities (arbitrary units) of the room-temperature XAS O $1s$ prepeak of LaNiO₃, PrNiO₃, and NdNiO₃.

	LaNiO ₃	PrNiO ₃	NdNiO ₃
Energy	528.4	528.6	528.8
Int. intensity	2.185	1.985	1.735

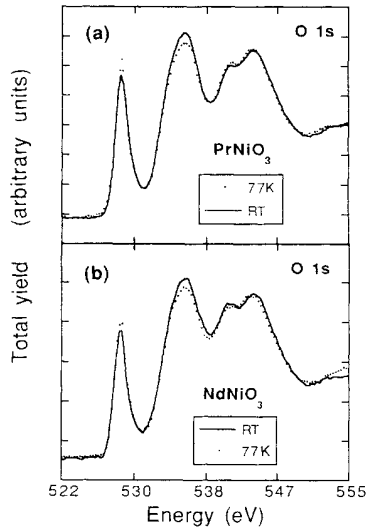


FIG. 3. O 1s edges of (a) PrNiO₃ and (b) NdNiO₃ at room temperature and $T=77$ K.

B. Ni $2p_{3/2-1/2}$ edges

According to the electric dipole selection rules, Ni $2p$ electrons may be excited into empty states either with $3d$ or $4s$ symmetry. The transitions $2p \rightarrow 3d$ are about 30 times stronger in intensity than $2p \rightarrow 4s$ transitions²⁴ due to the large overlap of the $3d$ wave functions with the $2p$ ones. Even if the Ni $2p$ XAS spectrum does not reproduce the details of the $3d$ unoccupied density of states, its integrated intensity is a measure of the total number of empty $3d$ states at the Ni sites.²⁵ In Fig. 4 the RT Ni $2p$ edges for the compounds PrNiO₃, NdNiO₃, and NiO are shown. The relatively weak Ni $2p_{3/2}$ structure in the LaNiO₃ spectrum appears in Fig. 6(a), overlaid by the very strong La $3d_{3/2} \rightarrow 4f$ transition. As can be clearly

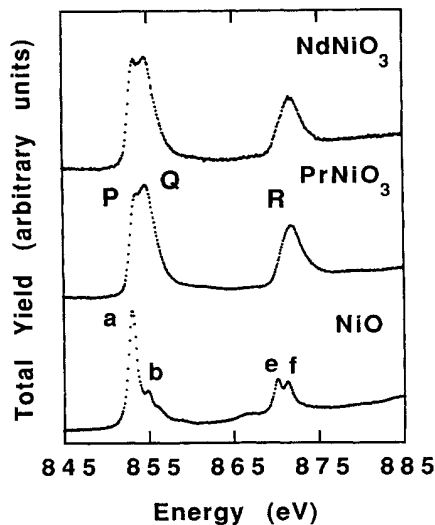


FIG. 4. Room-temperature Ni $2p_{3/2-1/2}$ edges of PrNiO₃, NdNiO₃, and NiO.

TABLE II. Absolute energies (eV) of the labeled features in the room-temperature XAS Ni $2p_{3/2-1/2}$ edges of NiO, PrNiO₃, and NdNiO₃.

	NiO		PrNiO ₃	NdNiO ₃
(a)	853.2	(P)	853.6	853.3
(b)	855	(Q)	854.9	854.9
(e)	870.3			
(f)	871.5	(R)	871.9	871.9

seen, the NiO spectrum is very different from the others. The RNiO₃ spectra show quite similar shapes, the only noticeable difference being the slightly higher intensity of the *P* feature in the Nd compound. In our opinion, this increase is due to the small amount of NiO (3% in weight) present in the sample. The fact that the energy of the NdNiO₃ *P* feature is (anomalously) closer to the NiO *a* feature (see Table II) also supports this assignment.

C. Ni 1s edge

In a dipolar transition, Ni 1s electrons can be excited into empty states of *p* symmetry. However, dipole-forbidden transitions can take place in some special circumstances. This is the case of the small structure at $E \approx 3$ eV present in the RNiO₃ Ni 1s edges, which has been identified as a $1s \rightarrow 3d$ quadrupolar transition²⁶ and whose integrated intensity may be correlated with the number of empty $3d$ states. Otherwise, the $4p$ states, which are totally empty in transition metals, are the lower dipole-allowed states reached by the photoelectron. Thus, the effects due to Ni $3d$ states are seen only indirectly.²⁷

Figure 5 shows the evolution of the Ni 1s edge spectra of PrNiO₃ and NdNiO₃ across the *M-I* transition. Because of the lack of mechanical movement of the energy-dispersive optics, we were able to measure with great accuracy the small differences observed between the low- and high-temperature spectra. Normalization, which was made after subtraction of the same linearly increasing background, was an easy task due to the minor changes observed in the absorption cross section. The zero energy corresponds, as is usually made in the analysis of the x-ray absorption edges, to the first inflexion point of the metallic Ni spectrum.

The evaluation of the energy positions of the labeled features shown in Fig. 5 was made by fitting the whole spectra (from -20 to 40 eV) with an arctangent plus three Lorentzians. The results are summarized in Table III. Figure 5 shows the existence of a change in the ab-

TABLE III. Absolute energies (eV), integrated intensities (arbitrary units), and FWHM (eV) of the *A* and *B* features in the room-temperature XAS Ni 1s edges of PrNiO₃ and NdNiO₃.

	(A) PrNiO ₃	(A) NdNiO ₃	(B) PrNiO ₃	(B) NdNiO ₃
Energy	17.0	17.0	24.6	24.6
Int. intensity	1589	1592	338	340
FWHM	3.66	3.68	3.66	3.68

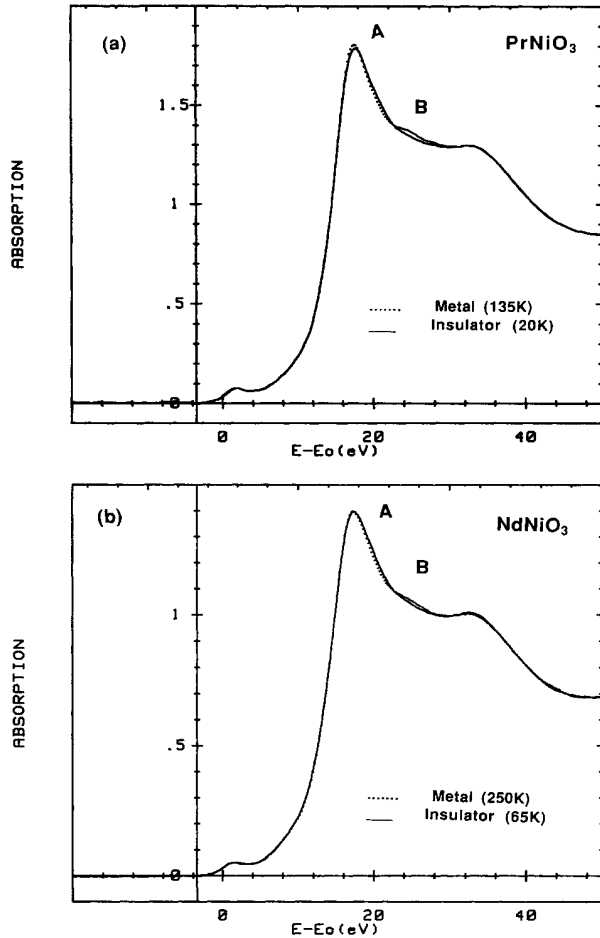


FIG. 5. Ni 1s edges of (a) PrNiO₃ and (b) NdNiO₃ in the metallic and insulating regimes.

sorption cross section at about the same temperature of the insulator to metal transition. This change consists of an decrease of the intensity in the region on the right of the *A* feature, and the simultaneous increase of the *B* feature. This is clearly shown by subtracting the high- and low-temperature spectra: the difference signal has two peaks separated by ≈ 5 eV, which is smaller than the refined difference between the *A* and *B* features (7.6 eV). For the sake of clarity, only two selected temperatures are displayed, but we would like to emphasize the fact that all the $T > T_{M-I}$ spectra and all the $T < T_{M-I}$ showed the same shape as the two representative curves displayed in Fig. 5. Moreover, the reported behavior was found to be reversible and perfectly reproducible.

D. Rare-earth (La, Pr, Nd) $3d_{5/2-3/2}$ edges

Figure 6 shows the measured RT La, Pr, and Nd $3d_{5/2-1/2}$ absorption edges, which probe the unoccupied density of *R* 4*f* states. The features present in the spectra are mainly due to the multiplet splitting of the quasi-

atomic initial and final states. The hypothesis that the effects coming from the environment of the rare earth can be considered as negligible is supported by several experimental works. These studies conclude that covalency effects are significant only for the first two rare earths in their tetravalent oxidation state (Ce^{4+} , Pr^{4+}).^{28,29} Thus, a comparison with the XAS edges of well-characterized materials can provide information on the valence of the rare earth in our compounds. Examining the La₂O₃, Pr₂O₃, and Nd₂O₃ electron-energy-loss spectroscopy (EELS) data reported by Alexander *et al.*,³⁰ we can conclude that all the rare earths are trivalent in the studied compounds.

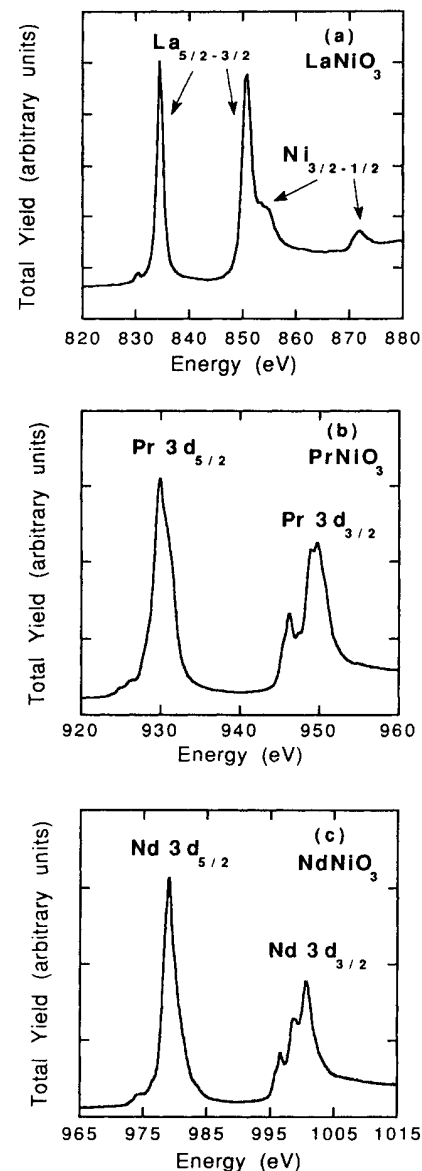


FIG. 6. Room-temperature $3d_{5/2-3/2}$ edges of (a) La in LaNiO₃, (b) Pr in PrNiO₃, and (c) Nd in NdNiO₃.

IV. DISCUSSION

A. O 1s edge

The main goal of this section is to discuss the origin of the sharp prepeak structure which appears at about 529 eV in the O 1s absorption edges. As discussed previously, several hypotheses can be considered to describe the ground state of these systems. Starting with a purely *ionic* point of view, that is, assuming spherical charge distributions localized around the atoms, we can write from a simple charge balance:

$$R^{3+}Ni^{3+}(O^{2-})_3. \quad (1)$$

This description is known to be highly crude and unrealistic. Several recent spectroscopic works on TM oxides show that a correct description of the electronic state of these compounds requires an explicit consideration of covalency.^{1,22,23} Though very different methods have been used in the literature to describe covalency effects, the most widely used among XAS spectroscopists is the configuration-interaction method. Within this formalism, the partial charge transfer from the anion to the cation is described by adding to the original ionic configuration an admixture of configurations in which one or more electrons have been transferred. In the RNiO₃ case, we can write the ground state of an "ionic" NiO₆ octahedral cluster as

$$|\Psi_{G_{\text{ionic}}}\rangle = |3d^7 2p^6\rangle, \quad (2)$$

and including covalency, as

$$|\Psi_{G_{\text{covalent}}}\rangle = \alpha|3d^7 2p^6\rangle + \beta|3d^8 \underline{L}\rangle + \gamma|3d^9 \underline{L}^2\rangle. \quad (3)$$

Here, $\alpha^2 + \beta^2 + \gamma^2 = 1$ and usually $\gamma \ll \beta < \alpha$. The values of α , β , and γ can in principle be obtained by combining the results of several x-ray spectroscopies. In the case of the RNiO₃ perovskites, it was pointed out in the Introduction the enormous importance of this information in order to decide the right framework within which the magnetic and transport properties must be explained. At the O 1s *K* edge, and allowing only intra-atomic XAS transition matrix elements, the intensity of the prepeak is proportional to β^2 and it is a measure of the covalency in the ground state. Thus, it should be very useful to compare the integrated intensities of the NiO and RNiO₃ prepeak because, for the first compound, several calculations of the degree of hybridization are available. Unfortunately, the presence of *R* 4*f* and 5*d* orbitals prevents a direct comparison because of the impossibility of performing a correct normalization. However, the intensity of the prepeak in RNiO₃ spectra is clearly very important, thus suggesting the existence of a highly covalent ground state. The results of magnetic neutron-diffraction experiments (Ni³⁺ low spin, $\mu_{Ni} = 1\mu_B$) implicitly support this finding. If the presence of 6 oxygen neighbors had a small effect in the electronic state of Ni, it should show the high-spin state of the free-ion configuration. The stabilization of the low-spin state is the signature of the existence of a crystal field due to the neighboring oxygens strong enough to overcome the first Hund's rule.

Though it is not possible to quantify the values of α and β without doing a full configuration-interaction calculation, we can estimate them using the well-known dependence of the Ni 3*d*-O 2*p* transfer integrals, T_{pd} , on the interatomic distance ($T_{pd} \sim \beta \sim 1/r^{3.5}$).³¹ This simple method is able to predict a degree of covalent mixing in TM oxides very close to the results obtained by more sophisticated calculations. A good example has been reported by van Elp⁸ for CoO and LiCoO₂. A cluster configuration-interaction calculation of the XPS and BIS spectra gives for CoO a ground state described as

$$|\Psi_G\rangle = \alpha|3d^7 2p^6\rangle + \beta|3d^8 \underline{L}\rangle + \gamma|3d^9 \underline{L}^2\rangle \quad (4)$$

with $\alpha^2 \approx 0.80$, $\beta^2 \approx 0.20$, and $\gamma^2 \approx 0$, and for LiCoO₂,

$$|\Psi_G\rangle = \alpha|3d^6 2p^6\rangle + \beta|3d^7 \underline{L}\rangle + \gamma|3d^8 \underline{L}^2\rangle, \quad (5)$$

with $\alpha^2 = 0.48$, $\beta^2 = 0.44$, and $\gamma^2 \approx 0.08$. Thus, the ratio between $\beta^2(\text{LiCoO}_2)$ and $\beta^2(\text{CoO})$ is ≈ 2.2 . From the knowledge of the Co-O distances (2.13 Å for CoO and 1.921 Å for (LiCoO₂) and using the $T_{pd} \sim \beta \sim 1/r^{3.5}$ dependence, we found $\beta^2(\text{LiCoO}_2) = 2.06 \beta^2(\text{CoO})$, which is in excellent agreement with the result of the reported calculations.

In NiO, Ni atoms are surrounded by six equivalent O atoms ($d_{Ni-O} = 2.090$ Å) and the ground state can be described as

$$|\Psi_G\rangle = \alpha|3d^8 2p^6\rangle + \beta|3d^9 \underline{L}\rangle + \gamma|3d^{10} \underline{L}^2\rangle \quad (6)$$

with approximately $\alpha^2 \approx 0.82$, $\beta^2 \approx 0.18$, and $\gamma^2 \approx 0$.⁸ In the RNiO₃ compounds, the four basal and the two apical O atoms of the NiO₆ octahedra are described by two different Wyckoff positions, but the six Ni-O distances are almost equal, differing only in a few thousandths of Å ($\langle d_{Ni-O} \rangle = 1.942$ Å for both PrNiO₃ and NdNiO₃). Thus, performing the same calculations as in the CoO and LiCoO₂ case, we find $\beta^2(\text{RNiO}_3) = 1.672 \times \beta^2(\text{NiO}) = 0.30$. Though it is only approximative, this result suggests that (a) the Ni 3*d*-O 2*p* hybridization in RNiO₃ is stronger than in NiO and (b) the weight of the 3*d*⁷ configuration is more important than the 3*d*⁸ \underline{L} one in the ground state of these compounds.

The intensity variations of the prepeak on going from La to Nd can be nicely correlated with changes in the Ni 3*d*-O 2*p* hybridization. Neutron-diffraction experiments indicate that, even if the Ni-O average distance is practically the same in all the compounds (1.933, 1.942, and 1.942 Å for La, Pr, and Nd, respectively, at RT), the Ni-O-Ni superexchange angle (φ) becomes smaller by reducing the size of the rare earth. Thus, $\varphi = 165.2^\circ$, 158.7° , and 157.1° for La, Pr, and Nd, respectively. Since a decrease of the superexchange angle implies a less-efficient overlap between Ni 3*d* and O 2*p* orbitals, the Ni 3*d*-O 2*p* hybridization is expected to be reduced on going from La to Nd. This is consistent with the observed diminution of the integrated prepeak intensity.

The origin of the small displacements in the prepeak positions (528.4, 528.6, and 528.8 eV for La, Pr, and Nd, respectively) is more difficult to interpret. In the insulating precursors of several high-*T_c* superconductors

(La₂CuO₄, La₂SrCu₂O₆, YBa₂Cu₃O₆, Nd₂CuO₄) a negative linear correlation between $d(\text{Cu-O}_{\text{basal}})$ and the energy threshold of this prepeak has been established.³⁰ This behavior has been explained in terms of the smaller covalency expected from a higher Cu-O distance, which supposes a better screening of the O 1s hole by the O 2p orbitals. In our case, the variation of covalency does not come from any distance variation, but from an angular variation. Thus, the former rule is probably not applicable. In any case, it is worth stressing that in other divalent Ni oxides, the energy of the prepeak does not seem to show any particular dependence on the Ni-O distance. Kuiper *et al.*² showed that in both NiO ($d_{\text{Ni-O}} = 2.090 \text{ \AA}$) and La₂NiO_{4+ δ} ($d_{\text{Ni-O basal}} = 1.932 \text{ \AA}$, $d_{\text{Ni-O apical}} = 2.20 \text{ \AA}$), the O 1s XAS prepeak appears at $E \approx 532 \text{ eV}$. In La₂NiO_{4+ δ} , polarized O 1s XAS measurements indicate that the intensity of the corresponding prepeak is mainly due to the O 2p_{x,y} and Ni $d_{x^2-y^2}$ hybridization, but its energy is the same as in NiO, even if in this compound the Ni-O_{basal} distance is about 8% larger. It would be very useful to have more experimental O 1s data in order to verify whether the behavior observed in NiO and La₂NiO_{4+ δ} can be extended to other formally divalent Ni oxides, but at the present time the origin of the different dependence of E_{prepeak} on the metal-O_{basal} distance in Cu and Ni oxides remains unclear.

B. Ni 2p edge

The two most remarkable facts of the NiO and RNiO₃ Ni 2p edges (see Fig. 4) are (a) the strong difference between the NiO and the RNiO₃ spectra and (b) the small shift (0.4 eV) of the perovskite edges to high energies (with respect to the NiO). The Ni 2p edges of divalent Ni compounds, as NiO or Ni dihalides, have been extensively studied during recent years.²³ The main features appearing in the spectra are quite similar in all the divalent compounds, and the presence of small satellites or the decrease of the multiplet splitting with smaller anion electronegativities are now well understood in terms of a covalent ground state of mainly Ni²⁺ ($3d^8$) character plus an anion-dependent fraction of the $3d^9\bar{L}$ and $3d^{10}\underline{L}^2$ configurations.

For Ni³⁺ compounds, both experimental results and theoretical calculations are quite scarce. To our knowledge, published Ni³⁺ spectra are inexistent (some unpublished results are, however, available)³² and the only theoretical calculations of the Ni³⁺ 2p XAS edge have been recently published by de Groot *et al.*³³ considering a pure $3d^7$ configuration. Two reasons explain this lack of information: first, the small number of Ni compounds which nominally show this high oxidation state (mainly due to the extreme synthesis conditions required to stabilize the 3⁺ valence) and second, the fact that configuration-interaction calculations including a full multiplet description are at the present time not a routine task, especially for intermediate ($3d^3$ to $3d^7$) transition metals.

Intuitively, the Ni³⁺ 2p edge will show a much richer multiplet structure and higher integrated intensity than Ni²⁺ due to its extra 3d hole. This is confirmed by de

Groot's calculations,³³ where Ni³⁺ *high-spin* spectra for different crystal-field splittings are reported. Our experimental data, which show much broader structures than NiO, can in principle be interpreted as corresponding to Ni³⁺. Unfortunately, the absence of fine structures does not allow a direct comparison with the available calculations. It should be noted that in this case, broadening is not due to the lack of experimental resolution. The quality of the NiO spectrum, obtained with the same experimental setup, is comparable with the data obtained in the Dragon monochromator,³⁴ thus indicating that the origin of the broadening is intrinsic to the sample.

In order to get additional information about the Ni 3d-O 2p hybridization, it is very interesting to compare the RNiO₃ spectra with the much more accessible Co²⁺ octahedrally coordinated experimental data. Due to the atomic origin of the main features appearing in the 2p absorption edges of 3d transition metals, we expect strong similarities between Co²⁺ and Ni³⁺ spectra due to their common $3d^7$ configuration.³³ Thus, looking at the data reported by Sette *et al.*³⁴ (see Fig. 7) for the Co 2p edge of the inverse spinel CoFe₂O₄[CoFe]{Fe}O₄, we found very similar structures which give us confidence in the validity of our hypothesis. A possible origin for the small differences between both spectra can be the different spin states of Co²⁺ (high spin in CoFe₂O₄) and Ni³⁺ (low spin in RNiO₃). Calculations including high- and low-spin states are necessary in order to establish their effect on the XAS spectra.

It is also very interesting to compare the Co 2p edges of CoFe₂O₄ and CoF₂ (rutile-type structure).³³ In both compounds Co²⁺ shows octahedral coordination and high-spin configuration ($t_{2g}^5 e_g^2$), but important differences between Co-O and Co-F bonds are expected due to the stronger electronegativity of the fluorine ion. Thus, covalency is expected to be more important in the oxide than in the fluoride. Looking at the spectra, the similarities between the Co 2p edges of both compounds are evident. However, the fine structure predicted by the atomic theoretical calculations is clearly visible only in the last one. Taking into account the more ionic nature of the Co-F bonding, we can tentatively establish a direct correlation between spectral smearing and covalency. Although this is only a very qualitative argument, it ex-

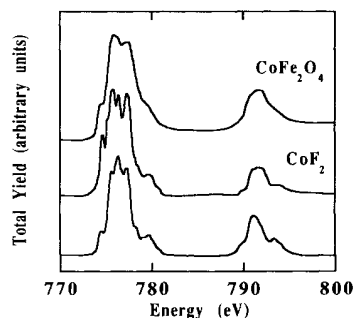


FIG. 7. Co 2p_{3/2-1/2} edges of CoFe₂O₄ (from Ref. 34) and CoF₂ (from Ref. 33). At the bottom, a calculation made by de Groot *et al.* (Ref. 33) including multiplet splitting and an octahedral crystal field is shown.

plains the smooth shape of the $RNiO_3$ spectra and gives additional support to the existence of a highly hybridized ground state in these compounds.

C. Ni K edge

It is well known that absorption edges are sensitive to the oxidation state of the absorbing atom. In general, the edge shifts to high energies when the oxidation state increases, due to the less-efficient screening of the core-hole potential. Much care needs to be taken in using this rule, due to the possible existence of superimposed effects coming from differences in the environment of the absorbing atoms.³⁵ It is, however, applicable for absorbers with the same coordination. A good example is the work of Crespin, Levitz, and Gatineau³⁶ made for the reduced forms of $LaNiO_3$.

Figure 8 shows the Ni 1s edge of Nd_2NiO_4 and $NdNiO_3$. In the first compound Ni is formally divalent, whereas in the second one, it shows a nominal 3+ oxidation state. Since in both compounds Ni ions are octahedrally coordinated, we can in principle apply the former rule. Some recent O 1s XAS experiments² indicate that the ground state of the NiO_6 octahedral clusters in the isostructural compound La_2NiO_4 is predominantly of $3d^8$ (Ni^{2+}) character. In view of the very similar Ni-O distances in both compounds ($d_{Ni-O\text{ basal}} = 1.9442 \text{ \AA}$, $d_{Ni-O\text{ apical}} = 2.235 \text{ \AA}$ for La_2NiO_4 and $d_{Ni-O\text{ basal}} = 1.9521 \text{ \AA}$, $d_{Ni-O\text{ apical}} = 2.231 \text{ \AA}$ for Nd_2NiO_4), we will suppose that NiO_6 units in Nd_2NiO_4 have roughly the same ground state. In order to make an estimation of the expected displacement in the Ni 1s edge due to variations in the Ni-O distance in a $\alpha|3d^8\rangle + \beta|3d^9\rangle$ (Ni^{2+}) compound, we have used the results obtained by some of us³⁷ with a single crystal of Pr_2NiO_4 . For this compound, which is isostructural with the two former nickelates ($d_{Ni-O\text{ basal}} = 1.9537 \text{ \AA}$, $d_{Ni-O\text{ apical}} = 2.221 \text{ \AA}$), XAS polarized measurements indicate that a difference of $d_{Ni-O\text{ apical}} - d_{Ni-O\text{ basal}} = 0.267 \text{ \AA}$ produces an energy shift in the Ni 1s edge of

1.8 eV. Single crystals of $RNiO_3$ and Nd_2NiO_4 are not available, but we can relate the energy shift of the edges in our powder data (3 eV) with the variation of average Ni-O distances (0.103 \AA). This simple calculation shows that the displacement to higher energies of the $NdNiO_3$ spectrum is much more important than that expected from such a distance reduction in a $\alpha|3d^8\rangle + \beta|3d^9\rangle$ compound. Thus, it is plausible to interpret the displacement as the signature of the $3d^7$ configuration.

Further experimental evidence supporting this conclusion is the high intensity of the forbidden quadrupolar transition in $NdNiO_3$. As pointed out in Sec. III C, the integrated intensity of this feature can be correlated with the total number of empty $3d$ states. If we consider purely ionic Ni^{2+} and Ni^{3+} , the ratio $[3d\text{ holes } (Ni^{3+})]/[3d\text{ holes } (Ni^{2+})] = 1.5$, which is roughly the same ratio than that found for the $NdNiO_3/Nd_2NiO_4$ integrated intensities.

V. METAL-INSULATOR TRANSITION

Many transition-metal compounds are known to exhibit a metal-insulator transition as a function of temperature, pressure, or chemical composition. In the first group, which includes $RNiO_3$ perovskites, the electronic localization is usually accompanied by structural distortions and/or magnetic ordering. These extra features can give additional insight about the nature of gap but, in general, the determination of the driving mechanism of the transition is not an easy task. A good example is NiS. This compound undergoes a first-order Pauli-metal to antiferromagnetic-semiconductor transition which is accompanied by an expansion of the unit cell.³⁸ In order to explain the opening of the gap, Mott-Hubbard,³⁹ antiferromagnetic,⁴⁰ and charge-transfer mechanism⁴¹ have been successively proposed.

A very different example is the $LnCoO_3$ perovskites ($Ln = La, Nd, Gd, Dy, Ho$).⁴² In this system, a very broad ($\approx 200 \text{ K}$) metal-semiconductor transition takes place for all the studied rare earths without any concomitant structural or magnetic effects. In this case, all authors agree with the interpretation of the electronic localization as a thermally driven low-spin to high-spin transition, due to the progressive overlap between the π^* ($O\ 2p - Ni\ t_{2g}$) valence band and σ^* ($O\ 2p - Ni\ e_g$) conduction band.^{43,44}

The experimental facts on $PrNiO_3$ and $NdNiO_3$ perovskites are very close to those observed in NiS: the metal-insulator transition is abrupt ($\approx 10 \text{ K}$), the associated structural changes are very small, and 3D antiferromagnetic order develops in the insulating state. Thus, the origin of the gap can in principle be magnetic, but this hypothesis must be considered with caution due to the separation between T_{M-I} and T_N in the compounds with smaller rare earths (Sm, Eu). In any case, it would be necessary to verify if, as it is the case in high- T_c superconductors, magnetic correlations are still present in the $T_N < T < T_{M-I}$ range.

Concerning the possibility of a Jahn-Teller or a Peierls distortion, polarized neutron-diffraction experiments²⁰ show that the small additional peaks which appear in the

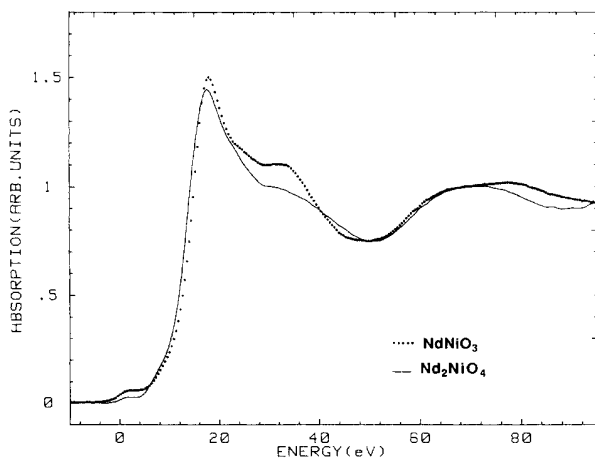


FIG. 8. Room-temperature Ni 1s edges of $NdNiO_3$ and Nd_2NiO_4 .

insulating state are *purely* magnetic. Thus, the structural changes simply consist in an enhancement of the orthorhombic distortion existing at higher temperatures. Moreover, the steric behavior of the structure across the *M-I* transition seems to indicate that the structural changes are not the *cause* but the *effect* of the electronic localization.¹²

Considering pure (not magnetic) electronic correlation, three kinds of gaps are envisageable: Mott-Hubbard type, charge-transfer type, and negative- Δ type. From the estimations made by Torrance *et al.*¹⁶ for the relative values of U and Δ , we can in principle disregard the Mott-Hubbard scheme. A negative- Δ mechanism seems also to be unlikely. The main reason is that it requires positive carriers (holes) in the metallic state, in contradiction with the results of the Seebeck coefficient measurements.⁴⁵ A charge-transfer gap looks, in principle, more suitable. It agrees with the estimations of Torrance *et al.* of U and Δ and, if the opening of the gap takes place because of a narrowing of the O $2p$ band,¹⁶ it is possible to have negative carriers in the metallic state. In order to test this hypothesis, we have compared the behavior of the Ni $1s$ and O $1s$ XAS spectra across the *M-I* transition with the one expected from the opening of such a gap. In this figure, the *A* and *B* features at the Ni $1s$ edges (see Fig. 4) have been tentatively interpreted as corresponding to the $1s \rightarrow 3d^8 \underline{L} 4p^1$ and $1s \rightarrow 3d^7 4p^1$, transitions, respectively. This assignment has been made by comparison with the Ni $1s$ XAS spectrum of the charge-transfer insulator Pr₂NiO₄. For this compound, which is isostructural with La₂NiO₄ and Nd₂NiO₄, polarized XAS measurements³⁷ allowed identification of the *A* and *B* features with the well-screened $1s \rightarrow 3d^9 \underline{L} 2p^1$ and poorly screened $1s \rightarrow 3d^8 4p^1$ transitions. The intensity ratio I_B/I_A and the energy separation of the features, $E_B - E_A$, can be written in terms of the charge-transfer energy Δ , the core-hole potential Q , and $T = \langle 3d^7 | H | 3d^8 \underline{L} \rangle$, the mixing between the $3d^7$ and $3d^8 \underline{L}$ configurations²³ as

$$I_B/I_A = \tan(\theta' - \theta), \quad E_B - E_A = [(Q - \Delta)^2 + 4T^2]^{1/2} \quad (7)$$

with $\tan(2\theta') = 2T/(\Delta - Q)$ and $\tan(2\theta) = 2T/\Delta$. It is reasonable to suppose that Δ and Q remain constant

across the metal-insulator transition. Therefore, any variation in the I_B/I_A ratio should be due to a change in the hybridization in the ground state (T). From the reported variation of the Ni-O distances and Ni-O-Ni angles, it is reasonable to assume a decreasing of T going from the metallic to the insulating regime. This implies a decrease in the weight of the $3d^8 \underline{L}$ configuration (*A* feature) going from the metallic to the insulating state. However, a clear increase of this feature is observed. The same conclusion can be derived from the analysis of the O $1s$ edges. The intensity of the prepeak, which is proportional to β^2 (the fraction of $3d^8 \underline{L}$ configuration), increases across the *M-I* transition, contrary to the behavior expected from the structural changes.

At present, we are not able to give a satisfactory explanation for this behavior. It would be very useful to carry out further experiments such as low-temperature Ni $2p$ XAS, which are expected to be more sensitive to the electronic changes in Ni than the Ni $1s$ and O $1s$ experiments. XPS and EPS measurements, which prove the full density of states in the valence band, may also be very helpful. Finally, some improvements should be made to the actual theories, as for example, the inclusion of effects associated with the appearance of the antiferromagnetic ground state.

VI. CONCLUSIONS

The reported XAS experiments on RNiO₃ perovskites have given some elements for the answer to the two main open questions concerning the electronic behavior of these compounds: the charge state of Ni and the mechanism of the metal-insulator transition. The results of the analysis of the O $1s$, Ni $2p$, and Ni $1s$ absorption edges indicate that the relevant electronic structure is well described in terms of a highly covalent ground state of mainly (70%) $3d^7$ character. A charge-transfer gap opening appears as the most likely mechanism to explain the electronic localization. However, it is very difficult to conciliate with the observed variations of the O $1s$ and Ni $1s$ edges across the transition. The last point indicates the limited scope of the actual theories, and shows that more-sophisticated mechanisms must be taken into account for further understanding of the metal-insulator transitions.

*Permanent address: Laboratory for Neutron Scattering, Eidgenössische Technische Hochschule Zürich, CH-5232 Villigen Paul Scherrer Institut, Switzerland.

†Permanent address: Laboratoire des Fluorures, Université du Maine, Avenue Olivier-Messiaen, 72017 LeMans CEDEX, France.

¹P. Kuiper, G. Kruizinga, J. Ghijsen, G. A. Sawatzky, and H. Verweij, *Phys. Rev. Lett.* **62**, 221 (1989).

²P. Kuiper, J. v. Elp, J. G. A. Sawatzky, A. Fujimori, S. Hosoya, and D. M. Leeuw, *Phys. Rev. B* **44**, 4570 (1991).

³D. D. Sarma, O. Strebel, C. T. Simmons, U. Neukirch, G. Kaindel, R. Hoppe, and H. P. Muller, *Phys. Rev. B* **37**, 9784

(1988).

⁴K. Allan, A. Campion, J. Zhou, and J. B. Goodenough, *Phys. Rev. B* **41**, 11 572 (1990).

⁵J. B. Goodenough, N. F. Mott, M. Pouchard, G. Demazeau, and P. Hagenmuller, *Mater. Res. Bull.* **8**, 647 (1973).

⁶Y. Takeda, S. Maka, M. Takano, T. Shinjo, T. Takada, and M. Shimada, *Mater. Res. Bull.* **13**, 61 (1978).

⁷P. K. Gallaguer, J. B. Macchesney, and D. N. E. Buchanan, *J. Chem. Phys.* **41**, 429 (1964).

⁸J. van Elp, Ph.D. thesis, University of Groningen, 1991.

⁹F. M. F. de Groot, Ph.D. thesis, University of Nijmegen, 1991.

¹⁰A. W. Webb, K. H. Kim, and C. Bouldin, *Solid State Com-*

- mun. **79**, 507 (1991).
- ¹¹G. R. Rao, M. S. Hedge, D. D. Sarma, and C. N. R. Rao, *J. Phys. Condens. Matter* **1**, 2147 (1989).
- ¹²J. L. García-Muñoz, J. Rodríguez-Carvajal, P. Lacorre, and J. B. Torrance, *Phys. Rev. B* **46**, 4414 (1992).
- ¹³F. Mehran, T. R. McGuire, J. F. Bringley, and B. A. Scott, *Phys. Rev. B* **43**, 11 411 (1992).
- ¹⁴J. B. Goodenough, D. G. Wickham, and W. J. Croft, *J. Phys. Chem. Solids* **5**, 107 (1958).
- ¹⁵J. Zaanen, G. A. Sawatzky, and J. W. Allen, *Phys. Rev. Lett.* **55**, 418 (1985).
- ¹⁶J. B. Torrance, P. Lacorre, C. Asavaroengchai, and R. M. Metzger, *J. Solid State Chem.* **90**, 168 (1991); J. Torrance, P. Lacorre, A. I. Nazzal, E. J. Ansaldo, and Ch. Niedermayer, *Phys. Rev. B* **45**, 8209 (1992).
- ¹⁷T. Mizokawa, H. Namatame, A. Fujimori, K. Akeyama, H. Kondoh, H. Kuroda, and N. Kosugi, *Phys. Rev. Lett.* **67**, 1638 (1991).
- ¹⁸P. Lacorre, J. B. Torrance, J. Pannetier, A. I. Nazzal, P. W. Wang, T. C. Huang, and R. L. Siemens, *J. Solid State Chem.* **91**, 225 (1991); J. K. Vasilio, M. Hornbostel, R. Ziebarth, and F. J. di Salvo, *J. Solid State Chem.* **81**, 208 (1989).
- ¹⁹I. D. Brown, in *Structure and Bonding in Crystals* (Academic, New York, 1981), Vol. 2.
- ²⁰J. L. García-Muñoz, J. Rodríguez-Carvajal, and P. Lacorre, *Europhys. Lett.* (to be published).
- ²¹M. Cyrot and C. Lyon-Caen, *J. Phys. (Paris)* **36**, 253 (1975).
- ²²H. Oda, Y. Yamaguchi, H. Takei, and H. Watanabe, *J. Phys. Soc. Jpn.* **42**, 101 (1977); A. E. Bocquet, A. Fujimori, T. Mizokawa, T. Saitoh, H. Namatame, S. Suga, N. Kimizuka, Y. Takeda, and M. Takano, *Phys. Rev. B* **45**, 1561 (1992).
- ²³G. van der Laan, J. Zaanen, G. A. Sawatzky, R. Karnatak, and J. M. Esteva, *Phys. Rev. B* **33**, 4253 (1986); J. Zaanen, C. Westra, and G. Sawatzky, *ibid.* **33**, 8060 (1986).
- ²⁴E. U. Condon and G. H. Shortley, *The Theory of Atomic Spectra* (Cambridge University Press, Cambridge, 1959).
- ²⁵J. Zaanen, G. A. Sawatzky, J. Fink, W. Speier, and J. C. Fuggle, *Phys. Rev. B* **32**, 4905 (1985).
- ²⁶J. E. Hahn, R. A. Scott, K. O. Hodgson, S. Doniach, S. R. Desjardins, and E. I. Solomon, *Chem. Phys. Lett.* **88**, 599 (1982).
- ²⁷H. Tolentino, E. Dartyge, A. Fontaine, T. Gourieux, G. Krill, M. Maurer, M.-F. Ravet, and G. Tourillon, *Phys. Lett. A* **139**, 474 (1989).
- ²⁸R. C. Karnatak, J. M. Esteva, H. Dexter, M. Gasgnier, P. E. Caro, and L. Albert, *Phys. Rev. B* **36**, 1745 (1987).
- ²⁹Ogasarawa, A. Kotani, K. Okada, and B. T. Thole, *Phys. Rev. B* **43**, 854 (1991).
- ³⁰M. Alexander, H. Romberg, N. Nücker, P. Adelmann, J. Fink, J. T. Markert, M. B. Maple, S. Uchida, H. Takagi, Y. Tokura, A. C. W. P. James, and D. W. Murphy, *Phys. Rev. B* **43**, 333 (1991).
- ³¹W. A. Harrison, *The Electronic Structure and Properties of Solids* (Freeman, San Francisco, 1980).
- ³²M. Verdaguer (private communication).
- ³³F. M. F. de Groot, M. Grioni, J. C. Fuggle, J. Ghijsen, G. A. Sawatzky, and H. Petersen, *Phys. Rev. B* **40**, 5715 (1989).
- ³⁴F. Sette, C. T. Chen, Y. Ma, S. Modesti, and N. V. Smith, in *X-Ray Absorption Fine Structure*, edited by F. S. Hafnain (Horwood, London, 1991); F. Sette and C. T. Chen, *Proceedings of the 2nd European Conference on Progress in X-Ray Synchrotron Radiation Research*, edited by A. Balerna, E. Berrieri, and S. Mobilio (SIF, Bologna, 1990).
- ³⁵M. Verdaguer, C. Cartier, M. Momenteau, A. Dartyge, A. Fontaine, G. Tourillon, and A. Mickalowick, *J. Phys. (Paris) Colloq.* **47**, C8-12 (1986).
- ³⁶M. Crespín, D. Levitz, and L. Gatineau, *J. Chem. Soc. Faraday Trans.* **79**, 1181 (1983).
- ³⁷H. Tolentino, M. Medarde, A. Fontaine, F. Baudelet, E. Dartyge, D. Guay, and G. Tourillon, *Phys. Rev. B* **45**, 8091 (1992).
- ³⁸J. Trahan, R. G. Goodrich, and S. F. Watkins, *Phys. Rev. B* **2**, 2859 (1970).
- ³⁹R. M. White and N. F. Mott, *Philos. Mag.* **24**, 845 (1971).
- ⁴⁰L. F. Mattheis, *Phys. Rev. B* **10**, 995 (1974).
- ⁴¹A. Fujimori, H. Namatame, M. Matoba, and S. Anzai, *Phys. Rev. B* **42**, 620 (1990).
- ⁴²X. Liu and C. T. Prewitt, *J. Phys. Chem. Solids* **52**, 441 (1991).
- ⁴³G. Thornton, I. W. Owen, and G. P. Diakun, *J. Phys. Condens. Matter* **3**, 417 (1991).
- ⁴⁴C. Thornton, B. C. Tofield, and D. E. Williams, *Solid State Commun.* **48**, 1213 (1982).
- ⁴⁵J. Fontcuberta (private communication).